

MAGNETOHYDRODYNAMICS OF GAMMA-RAY BURST OUTFLOWS

NEKTARIOS VLAHAKIS¹ AND ARIEH KÖNIGL

Department of Astronomy & Astrophysics and Enrico Fermi Institute, University of Chicago,
 5640 S. Ellis Ave., Chicago, IL 60637
 vlahakis@jets.uchicago.edu, arieh@jets.uchicago.edu

Accepted by ApJL, 2001 November 13

ABSTRACT

Using relativistic, axisymmetric, ideal MHD, we examine the outflow from a disk around a compact object, taking into account the baryonic matter, the electron-positron/photon fluid, and the large-scale electromagnetic field. Focussing on the parameter regime appropriate to γ -ray burst outflows, we demonstrate, through exact self-similar solutions, that the thermal force (which dominates the initial acceleration) and the Lorentz force (which dominates further out and contributes most of the acceleration) can convert up to $\sim 50\%$ of the initial total energy into asymptotic baryon kinetic energy. We examine how baryon loading and magnetic collimation affect the structure of the flow, including the regime where emission due to internal shocks could take place.

Subject headings: gamma rays: bursts — ISM: jets and outflows — MHD — methods: analytical — relativity

1. INTRODUCTION

Cosmological gamma-ray bursts (GRBs) evidently involve the emission of the isotropic equivalent of $\sim 10^{51} - 10^{54}$ ergs on a typical time scale of a few seconds in the vicinity of a newly formed stellar-mass black hole or rapidly rotating neutron star (see reviews by Piran 1999 and Mészáros, Rees, & Wijers 1999). To avoid strong attenuation of the γ -rays by pair-production interactions with lower-energy photons (the “compactness” problem), the Lorentz factor γ of the emitting gas must exceed $\sim 10^2 - 10^3$. The most natural way of powering the burst seems to be the conversion of the kinetic energy of the relativistic outflow into nonthermal (most likely synchrotron) radiation. Because of the high initial energy density and characteristic photon energy, the dynamical evolution of GRBs has traditionally been modeled in terms of the expansion of an initially opaque electron-positron (e^\pm) fireball. Although a pure- e^\pm fireball could in principle attain $\gamma \gtrsim 10^3$ in the optically thin region where the observed emission must originate, the fraction of the energy carried by pairs would be only $\sim 10^{-5}$ (Grimsrud & Wasserman 1998). If, however, the fireball contains enough baryons (of total mass M_b) that it becomes “matter dominated” before it gets optically thin, then most of its initial (suffix i) energy \mathcal{E}_i is converted into bulk kinetic energy of baryons (with asymptotic Lorentz factors $\gamma_\infty \approx \mathcal{E}_i/M_b c^2$) instead of escaping as radiation. Baryon loading of the fireball at the source is expected in view of the highly super-Eddington luminosity involved, and viable models in fact face the issue of why it is not so efficient as to render γ_∞ too low (the “baryon contamination” problem).

According to currently accepted GRB formation scenarios, the burst is powered by the extraction of rotational energy from the central black hole or neutron star, or, alternatively, from the debris disk left behind when the mass near the origin collapses into a black hole. In either case, strong ($\gtrsim 10^{14}$ G) magnetic fields provide the most plausible means of extracting the energy \mathcal{E}_i on the burst time scale. If the field were initially weaker, it would likely be rapidly amplified by differential rotation or dynamo action to the requisite strength. The magnetic energy might be dissipated near the origin in a series of flares, giving rise to a “magnetic” fireball (e.g., Narayan, Paczyński, &

Piran 1992; Mészáros, Laguna, & Rees 1993). Alternatively, the magnetic field may have a large-scale, ordered component that could help guide and collimate the outflow, and, if it is strong enough, also contribute to its acceleration (e.g., Usov 1994; Thompson 1994; Mészáros & Rees 1997; Katz 1997). Even if the flow is not magnetically driven, the field may be strong enough to account for the observed synchrotron emission (Sruuit, Daigne, & Drenkhahn 2001). Magnetic collimation is, in fact, consistent with the observational indications for GRB jets (e.g., Sari, Piran, & Halpern 1999) and could be very helpful in reducing the source energy requirements to plausible values. Furthermore, if the outflow is largely Poynting flux-dominated, then the implied lower radiative luminosity near the origin could alleviate the baryon contamination problem. Magnetic fields have thus come to be regarded as the favored means of driving GRB outflows.

The purpose of this Letter is to provide an overview of the magnetohydrodynamics (MHD) of GRB outflows, clarifying the relationship between the thermal (fireball) and Lorentz accelerations, identifying the parameter regimes where qualitatively different behaviors are expected, and demonstrating that the observationally inferred properties of these outflows can be attributed to magnetic driving. A detailed exposition of the semianalytic solutions on which this overview is based is given in N. Vlahakis & A. Königl, in preparation (hereafter VK).

2. THE MHD DESCRIPTION

For the purpose of illustration, we assume that the outflow originates in a debris disk around a stellar-mass black hole (e.g., Mészáros & Rees 1997; Fryer, Woosley, & Hartmann 1999). In light of the considerations of §1, we concentrate on the case of a magnetically driven, axial jet that has a sufficiently high baryon loading to insure that it is matter dominated when it becomes optically thin (see §4), and in which a significant fraction of the Poynting flux is eventually converted into kinetic energy. As discussed by Sruuit et al. (2001), such configurations can be validly described by the MHD approximation on the spatial scales of interest, and, furthermore, they are not expected to dissipate a substantial amount of magnetic energy along the way. Correspondingly, we adopt the equations of relativistic, ideal

¹ McCormick Fellow.

MHD to describe the flow. We anticipate that, near the origin, the thermal energy associated with the radiation and e^\pm pairs is nonnegligible and that the optical depth is large enough to ensure local thermodynamic equilibrium. We therefore assume that the gas (consisting of baryons with their neutralizing electrons as well as of photons and pairs) evolves adiabatically with a polytropic index of 4/3. Assuming a quasi-steady poloidal magnetic flux function A and changing variables from (A, ℓ, t) to $(A, \ell, s = ct - \ell)$, with ℓ the arclength along a poloidal field-line, it can be shown that all terms with derivatives with respect to s are negligible when the flow is highly relativistic. As is elaborated on in VK, the equations are then effectively time independent and the motion can be described as a frozen pulse whose internal profile is specified through the variable s (see also Piran 1999). We discuss time-dependent effects in §6.

Assuming also axisymmetry, the full set of MHD equations can be partially integrated to yield several field-line constants: the mass-to-magnetic flux ratio $\Psi_A(A, s)$, the field angular velocity $\Omega(A, s)$ (which equals the matter angular velocity at the footpoint of the field line in the disk), the total (kinetic + magnetic) specific angular momentum $L(A, s)$, the total energy-to-mass flux ratio $\mu(A, s)c^2$, and the adiabat $Q(A, s) \equiv P/\rho_0^{4/3}$ (where ρ_0 and P are, respectively, the rest-mass density and total gas pressure measured in the fluid frame). Two integrals remain to be performed, involving the Bernoulli and trans-field force-balance equations. There are correspondingly two unknown functions, which we choose for convenience to be $x \equiv \bar{\omega}\Omega/c$, the radial distance of the field line [in cylindrical coordinates $(z, \bar{\omega}, \phi)$] in units of the “light cylinder” radius, and the “Alfvénic” Mach number $M \equiv \sqrt{4\pi\rho_0\xi(\gamma V_p/B_p)} = \Psi_A \sqrt{\xi/4\pi\rho_0}$ (where ξ is the enthalpy-to-rest energy ratio, and where V_p and B_p are the poloidal components of the velocity and magnetic field, respectively, measured in the central object’s frame). The solutions derived in VK are obtained under the most general ansatz for radial self-similarity [in spherical coordinates (r, θ, ϕ)], in which the shape $r(\theta, A)$ of the poloidal field lines is given as a product of a function of A times a function of θ : $r = \mathcal{F}_1(A)\mathcal{F}_2(\theta)$ (or, equivalently, $A = \mathcal{A}[\bar{\omega}/G(\theta)]$; Vlahakis & Tsinganos 1998).

Initially, the outflow evolves as a fireball: it expands isotropically in the comoving frame, with the large-scale field only acting as a guide (e.g., Mészáros et al. 1993). If the baryon loading is large enough, this continues until all the thermal energy of the radiation field and the pairs is transformed into kinetic energy of the baryons. Subsequently, the Lorentz force converts Poynting flux into baryon kinetic energy, and it also collimates the flow. The Lorentz force remains dominant (implying that the field is force free) all the way to the point where the kinetic energy of the baryons becomes comparable to the electromagnetic energy. We assume that the asymptotic shape of the flow is cylindrical and that the final stage is characterized by an equipartition between the Poynting and kinetic energy fluxes. (The latter assumption is motivated by the exact “cold” solutions of Li, Chiueh, & Begelman 1992.) The transition from a parabolic to a cylindrical shape occurs far downstream from the Alfvén point ($\theta \ll 1$), where the ratio of the kinetic energy flux $\xi\gamma^2\rho_0c^3$ to the Poynting flux $cEB_\phi/4\pi$ (where E is the electric field amplitude) equals M^2/x^2 . If ϑ is the (small) opening half-angle of the outflow, then $|\nabla A| \sin(\theta - \vartheta) = \partial A/\partial r$. Substituting this into the Bernoulli equation, we find the slope of

the field lines

$$\left(\frac{d \ln \bar{\omega}}{d \ln z}\right)_A = \frac{\vartheta}{\theta} = 1 - \left(1 + \frac{M^2}{x^2}\right) \frac{\sigma}{\mu} \frac{r}{A} \left(\frac{\partial A}{\partial r}\right)_\theta, \quad (1)$$

where $\sigma \equiv A\Omega^2/(c^3\Psi_A)$ is the magnetization parameter. Equipartition between the Poynting and kinetic energy fluxes ($M^2 = x^2$) in the final cylindrical stage ($d\bar{\omega} = 0$) means that $r\partial A(r, \theta)/\partial r = \mu/(2\sigma)$. Substituting this into equation (1) and specializing to the force-free ($M^2 \ll x^2$) parabolic regime, gives $d \ln z/d \ln \bar{\omega} = 2$, so the shape of the force-free field lines is $z/\bar{\omega}_i = (\bar{\omega}/\bar{\omega}_i)^2/(2 \tan \vartheta_i)$, with ϑ_i the initial opening half-angle (cf. Contopoulos 1995).

3. SCALING LAWS

Beyond the light surface (which is close to the Alfvén surface, since the flow is nearly force free), the large-scale electromagnetic field is given by

$$(B_z, B_\theta, B_\phi, E_z, E_\theta, E_\phi) = \frac{\mu c \Psi_A}{x} \left(\frac{1}{x}, \frac{\bar{\omega}}{2xz}, -1, \frac{\bar{\omega}}{2z}, -1, 0 \right). \quad (2)$$

The comoving field amplitude satisfies $B_{co}^2 = B^2 - E^2$ (a Lorentz invariant) and $B_{co}^2 \approx B_p^2 + B_\phi^2/\gamma^2 \ll B_p^2$, which together imply $B_\phi \approx E_\theta$ (or, equivalently, $L\Omega \approx \mu c^2$).

We approximate the outflow as a pair of shells that move in opposite directions from the debris disk, each having an initial meridional cross section $(\Delta z)_i \times (\Delta \bar{\omega})_i$, with $(\Delta \bar{\omega})_i = 10^6(\Delta \bar{\omega})_{i,6}$ cm comparable to $\bar{\omega}_i = 10^6\bar{\omega}_{i,6}$ cm (the mean radius of the debris disk) and $(\Delta z)_i \approx c\Delta t = 3 \times 10^{11}\Delta t_1$ cm (where $\Delta t = 10\Delta t_1$ s is the total duration of the burst). The total baryonic mass of outflowing matter is $M_b = 4\pi\bar{\omega}_i(\Delta \bar{\omega})_i(\Delta z)_i\gamma_i\rho_{0i} = 2 \times 10^{-7}\gamma_i\rho_{0i,2}\bar{\omega}_{i,6}(\Delta \bar{\omega})_{i,6}\Delta t_1 M_\odot$, where $\rho_{0i} = 10^2\rho_{0i,2}$ g cm⁻³. The total energy is $\mathcal{E}_i = \mu M_b c^2 = 4 \times 10^{51}(\mu/10^4)\gamma_i\rho_{0i,2}\bar{\omega}_{i,6}(\Delta \bar{\omega})_{i,6}\Delta t_1$ ergs, and initially it resides predominantly in the electromagnetic field; the initial thermal energy (associated with the enthalpy of the photons and pairs) is $\xi_i M_b c^2 = (\xi_i/\mu)\mathcal{E}_i$.

The constancy of the mass-to-magnetic flux ratio $\Psi_A = 4\pi\rho_0\gamma V_p/B_p$ and equation (2) imply

$$\gamma\rho_0\bar{\omega}^2 = \gamma_i\rho_{0i}\bar{\omega}_i^2. \quad (3)$$

If Θ is the temperature in units of the electron rest energy, then, by the conservation of specific entropy along the flow, $P/(\rho_0\Theta) = \text{const}$, or (since $P \propto \Theta^4$)

$$\rho_0 = \rho_{0i}(\Theta/\Theta_i)^3. \quad (4)$$

Energy flux conservation, in turn, gives

$$\xi\gamma - (\bar{\omega}\Omega B_\phi/\Psi_A c^2) = \mu. \quad (5)$$

So long as $\xi > 1$ (the fireball phase), $\xi \propto \Theta$. Also, by equation (5), $\xi\gamma$ is constant since the specific Poynting flux does not vary along the flow for a force-free field. Equations (3)–(5) thus imply

$$\gamma = \gamma_i(\bar{\omega}/\bar{\omega}_i), \quad \rho_0 = \rho_{0i}(\bar{\omega}_i/\bar{\omega})^3, \quad \Theta = \Theta_i(\bar{\omega}_i/\bar{\omega}). \quad (6)$$

These scalings are the same as in a spherically symmetric, hydrodynamic (HD) fireball, except that the cylindrical radius $\bar{\omega}$ replaces the spherical radius r in the magnetically guided case.

Beyond the point where $\xi = 1$, magnetic acceleration takes over and the Lorentz factor continues to increase until the cylindrical regime ($\bar{\omega} = \bar{\omega}_\infty$) is reached. The magnetic acceleration is associated with a small (linear in $\bar{\omega}$) deviation of the Poynting flux from its force-free value,

$$-(\bar{\omega}\Omega B_\phi/\Psi_A c^2) = \mu - (\bar{\omega}/\bar{\omega}_i). \quad (7)$$

By combining equation (7) with equations (5) and (3), it is seen that the scalings of γ and ρ_0 with $\bar{\omega}$ given by equation (6) are

maintained also in the magnetic acceleration zone. In fact, since the density in the central object's frame is $\gamma\rho_0 = \gamma_i\rho_{0i}(\bar{\omega}_i/\bar{\omega})^2$ and the $\bar{\omega}$ -width of the shell (given the parabolic shape of the field lines) evolves as $\Delta\bar{\omega}/(\Delta\bar{\omega})_i = \bar{\omega}/\bar{\omega}_i$, mass conservation implies that, while the flow continues to expand isotropically in the comoving frame, the width of the shell remains constant [$\Delta z = (\Delta z)_i$] in the central source's frame (consistent with the frozen-pulse approximation).

4. BARYON LOADING

Two parameters determine the basic character of the flow: The first is the initial enthalpy of the flow in units of the rest energy of the baryonic component, $\xi_i = 400\Theta_i^4(\rho_{0i,2})^{-1}$, where we approximate the initial radiation field by a blackbody distribution and the e^\pm pairs by a Maxwellian distribution. The second is the initial Poynting flux in units of the baryon rest-energy flux. As we focus on Poynting flux-dominated outflows, this ratio is $\mu - \xi_i \approx \mu$.

Initially the flow is optically thick. The distance where it becomes optically thin is determined by ξ_i . The pertinent regimes of this parameter were previously analyzed for the case of a radially expanding HD fireball (see Piran 1999). We now adapt this analysis to the present (nonradial) geometry.

The opacity has two contributions: one due to pairs (τ_\pm) and another due to the electrons that neutralize the baryons (τ_b). As the flow expands, its temperature decreases. When $\Theta \approx 0.04$, the pair number density becomes negligible and the opacity from there on is determined by the neutralizing electrons. For the radiation-dominated case, $\tau_b < 1$ at that point, corresponding to $\xi_i > \xi_{i\pm}$ (with $\xi_{i\pm} = 2.5 \times 10^7 \Theta_i^2 (\Delta\bar{\omega})_{i,6}^{-1}$). If $\xi_i < \xi_{i\pm}$, the flow continues to be optically thick until $\tau_b = 1$. If at that point the radiation energy density exceeds the baryon rest-energy density, then one is still in the radiation-dominated regime. This corresponds to $\xi_i > \xi_{ib}$, with $\xi_{ib} = 6 \times 10^3 \Theta_i^{4/3} (\Delta\bar{\omega})_{i,6}^{1/3}$. For $\xi_i < \xi_{ib}$, the flow is matter dominated when it becomes optically thin. Finally, $\xi_i \approx 1$ correspond to the cold limit. Since magnetic acceleration now plays a role, the outflow is not necessarily nonrelativistic in this limit: only if $\mu \approx 1$ also holds will the flow be Newtonian. The most plausible regime for GRB outflows is $1 < \xi_i < \xi_{ib}$, and we adopt it from here on.

5. STRUCTURE OF THE FLOW

As the flow moves outward it passes through the following points (see Fig. 1):

1. $\bar{\omega}_1 = \bar{\omega}_i$: origin of the outflow, $\gamma_i \approx 1$.
2. $\bar{\omega}_2 = \bar{\omega}_i \sqrt{3/2}$: slow-magnetosonic surface, $V_p \approx c/\sqrt{3}$.
3. $\bar{\omega}_3 = c/\Omega$: Alfvén (\approx light) surface.
4. $\bar{\omega}_4 = (c/\Omega)\sqrt{\mu/\xi_i}$: classical fast-magnetosonic surface, $\gamma V_p \approx \sqrt{(B^2 - E^2)/(4\pi\rho_0\xi)}$. Unlike the purely radial case (Michel 1969), this point is located at a finite distance from the origin. The bulk of the magnetic acceleration occurs downstream from this point through the “magnetic nozzle” mechanism (Li et al. 1992). In essence, this term is a shorthand for the fact that an MHD flow can continue to accelerate until it crosses the modified fast-magnetosonic singular surface.² This effect is not purely relativistic: it is manifested in an exact solution of the nonrelativistic MHD equations where all the singular surfaces (including the modified-fast one) are crossed (Vlahakis et al. 2000), and there, too, most of the acceleration

occurs downstream of the classical fast-magnetosonic surface (but *upstream* of the modified-fast surface).

5. $\bar{\omega}_5 = 25\Theta_i\bar{\omega}_i$: $\tau_\pm = 1$.
6. $\bar{\omega}_6 = \xi_i\bar{\omega}_i$: end of thermal acceleration, $\gamma \approx \xi_i$. The entire initial thermal energy of the photons and pairs has by this point been converted into baryon kinetic energy. Magnetic acceleration effectively starts here.
7. $\bar{\omega}_7 = 5 \times 10^3 (\Delta\bar{\omega})_{i,6}^{1/2} \rho_{0i,2}^{1/2} \bar{\omega}_i$: $\tau = \tau_b = 1$, the flow becomes optically thin to Compton scattering.
8. $\bar{\omega}_8 = \bar{\omega}_\infty \approx (\mu/2)\bar{\omega}_i$: cylindrical flow regime. Near-equipartition between the Poynting and the baryon kinetic-energy fluxes is attained, with $\gamma = \gamma_\infty \approx \mu/2$.

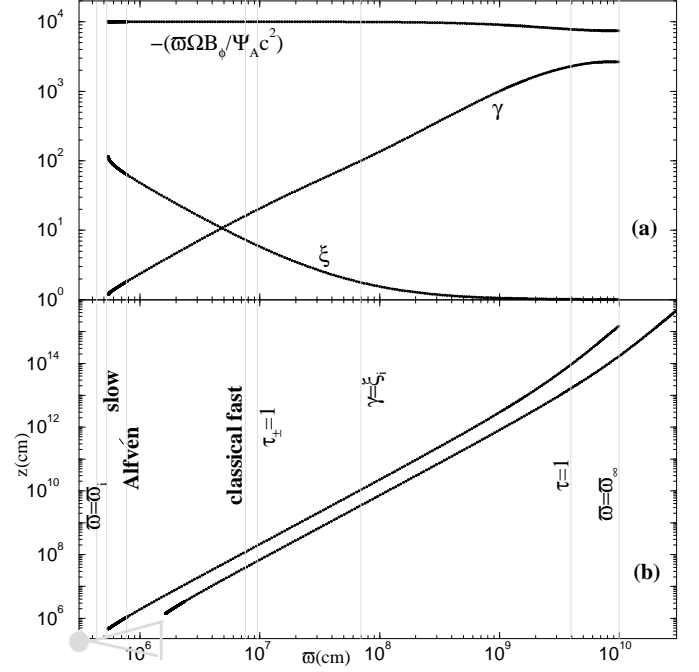


FIG. 1.— Exact self-similar solution of the relativistic MHD equations, illustrating the GRB outflow structure discussed in this Letter. (a) The Lorentz factor γ , the ratio ξ of the enthalpy to the rest energy, and the ratio of the Poynting flux to the rest-energy flux (top curve) are shown as functions of $\bar{\omega}$, the distance from the axis of rotation, along the innermost field line. (b) The meridional projections of the innermost and outermost field lines are shown on a logarithmic scale, along with a sketch of the black-hole/debris-disk system. The vertical lines mark the positions of the various transition points listed in §5 along the innermost field line.

The inequalities $\bar{\omega}_1 < \bar{\omega}_2 < \bar{\omega}_3 < \bar{\omega}_4 < \bar{\omega}_8$ always hold, as do, in the regime of interest, $\bar{\omega}_5 < \bar{\omega}_7$ (valid for $\xi_i < \xi_{i\pm}$) and $\bar{\omega}_6 < \bar{\omega}_7$ (valid for $\xi_i < \xi_{ib}$). The validity condition for the inequality $\bar{\omega}_7 \lesssim \bar{\omega}_8$, which expresses the requirement that the flow be optically thin to Compton scattering in its final (cylindrical) stage, corresponds to an upper bound on the baryon loading: $\rho_{0i,2} \lesssim (\mu/10^4)^2 (\Delta\bar{\omega})_{i,6}^{-1}$ [or $\rho_{0i,2} \lesssim 0.4(\Delta\bar{\omega})_{i,6}^{-1} \bar{\omega}_{i,6}^{-2/3} (\Delta t_1)^{-2/3} (\xi_i/10^{51} \text{ ergs})^{2/3}$]. We note, however, that the increase of γ with $\bar{\omega}$ is slower than linear as the cylindrical regime is approached (see Fig. 1), which implies that $\bar{\omega}_\infty$ is larger than $(\mu/2)\bar{\omega}_i$ and the actual upper bound on the initial baryon mass density is larger than the analytic estimate (typically by a factor of a few).

All of the above points are indicated in Figure 1, where an illustrative solution of the steady, relativistic MHD equations is presented. The figure demonstrates the validity of the

² The modified (and *not* the classical) fast-magnetosonic surface is a singular surface for the steady MHD equations when one solves simultaneously the Bernoulli and transfield equations (e.g., Bogovalov 1997).

scaling $\gamma \approx \bar{\omega}/\bar{\omega}_i$ over several decades in $\bar{\omega}$ and the separation of the thermal ($\gamma < \xi_i$) and magnetic ($\gamma > \xi_i$) acceleration regimes. It also manifests the significant collimation from the comparatively large initial opening half-angle ($\vartheta_i \approx 24^\circ$) to a very nearly cylindrical geometry (attained on scales $\gtrsim 10^{14}$ cm from the origin). Equation (7) for the Poynting flux is also verified. It is, furthermore, seen that approximate equipartition ($\gamma \approx -\bar{\omega}\Omega B_\phi/\Psi_A c^2$) holds during the final phase of the flow.

6. APPLICATION TO GRBs

To demonstrate how the model outflows discussed in §5 could account for observed GRBs, we adopt as fiducial source parameters a γ -ray fluence of $\sim 10^{-5}$ ergs s^{-1} and a distance ~ 3 Gpc, which imply an isotropic equivalent energy of $\sim 10^{53}$ ergs. If the γ -ray emitting material is in fact confined to a pair of cones of opening half-angle $\sim 3^\circ$, then the actual radiated energy is $\sim 1.5 \times 10^{50}$ ergs. As we noted in §1, the emission is believed to be powered by the kinetic energy of the relativistic outflow, and the most common interpretation is in terms of internal shocks produced by the collision of overtaking shells (see Piran 1999). Assuming that the kinetic-to-radiative energy conversion efficiency is $\sim 10\%$ and that the magnetic stresses can transfer as much as $\sim 1/2$ of the initial energy into baryon kinetic energy, we infer $\mathcal{E}_i \approx 3 \times 10^{51}$ ergs. If the energy is deposited in the form of a Poynting flux over $\Delta t \approx 10$ s, then the field at the origin must be $\sim (\mathcal{E}_i c / \bar{\omega}_i^3 (\Delta \bar{\omega})_i \Delta t \Omega^2)^{1/2} \approx 3 \times 10^{14}$ G for $\bar{\omega}_i \approx (\Delta \bar{\omega})_i \approx 10^6$ cm and $\Omega \approx 10^4$ s $^{-1}$ (representative of a debris disk that extends to the last stable orbit of a rotating solar-mass black hole). To satisfy the constraint $\bar{\omega}_7 \lesssim \bar{\omega}_8$ (see §5), the maximum baryonic rest-mass density is $\rho_{0i,2} \approx 1$. In the solution presented in Figure 1, we adopted as a plausible temperature $\Theta_i \approx 1/\sqrt{2}$, corresponding to $\xi_i \approx 100$.

The variability properties of the observed GRBs have been interpreted in terms of $N = 100 N_2$ distinct shells that are ejected with slightly different Lorentz factors and whose subsequent collisions give rise to the “internal” shocks responsible for the γ -ray emission (e.g., Piran 1999). Adopting $\gamma \propto \bar{\omega} \propto \sqrt{z}$, one may integrate the equation of motion for each shell and show that two neighboring shells starting with $\Delta\gamma_i \sim 1$ will

not collide for as long as they move in the flow acceleration zone. Only after the shells reach the constant-velocity, cylindrical flow regime, will the two shells collide (at a height $z_f \approx \gamma_\infty^2 (\Delta z)_i / N = 7.5 \times 10^{16} (\mu/10^4)^2 \Delta t_1 / N_2$ cm, assuming an initial separation $\sim (\Delta z)_i / N$). A lower bound on the Lorentz factor in this region can be obtained from the requirement that the optical depth to photon-photon pair production be less than 1: $\gamma \gtrsim 10^3 \epsilon_{t,1}^{1/4} N_2^{1/4} (\Delta t_1)^{-1/4} (1+z_r)^{1/4} H_{65}^{-1/2}$, where $\epsilon_{t,1}$ GeV is the energy of a test photon, $65 H_{65}$ km s $^{-1}$ Mpc $^{-1}$ is the Hubble constant, and z_r is the redshift (Woods & Loeb 1995). The solution exhibited in Figure 1 demonstrates that magnetically accelerated flows can attain the requisite high values of γ .

Although our analysis can be generalized to arbitrary magnetic field configurations, we have concentrated on the self-similar form for which we have exact solutions of the MHD equations (see VK). Real GRB outflows evidently have a finite opening half-angle (estimated to be at least 5° on average; Mészáros et al. 1999), and thus are not accurately represented by our asymptotically cylindrical solutions. This discrepancy should not, however, affect our basic conclusions about the robustness of the magnetic acceleration mechanism for these flows. It remains a challenge for future work to find exact solutions with conical asymptotics. We note in this connection that, although the outflowing “shells” conceivably do not fill the entire solid angle into which they are ejected, the internal shock mechanism requires that multiple shells be ejected along any given direction (e.g., Kumar & Piran 2000). The guiding property of a magnetic field in an MHD-driven outflow provides a natural physical basis for this picture.

In conclusion, we have shown that ordered magnetic fields can transform up to $\sim 50\%$ of the energy deposited by the central source of a GRB into kinetic energy of a collimated flow of baryons with $\gamma \sim 10^3$. This energy, in turn, may be converted into radiation by internal shocks.

We thank J. Granot for helpful conversations. This work was supported in part by NASA grant NAG 5-9063 and by DOE under Grant No. B341495.

REFERENCES

- Bogovalov, S. V. 1997, A&A, 323, 634
 Contopoulos, J. 1995, ApJ, 446, 67
 Fryer, C. L., Woosley, S. E., & Hartmann, D. H. 1999, ApJ, 526, 152
 Grimsrud O. M., & Wasserman I. 1998, MNRAS, 300, 1158
 Katz, J. I. 1997, ApJ, 490, 633
 Kumar, P., & Piran, T. 2000, ApJ, 535, 152
 Li, Z.-Y., Chiueh, T., & Begelman, M. C. 1992, ApJ, 394, 459
 Mészáros, P., Laguna, P., & Rees, M. J. 1993, ApJ, 415, 181
 Mészáros, P., & Rees, M. J. 1997, ApJ, 482, L29
 Mészáros, P., Rees, M. J., & Wijers, R. 1999, NewA, 4, 303
 Michel, F. C. 1969, ApJ, 158, 727
 Narayan, R., Paczyński, B., & Piran, T. 1992, ApJ, 395, L83
 Piran, T. 1999, Physics Reports, 314, 575
 Sari, R., Piran, T., & Halpern, J. P. 1999 ApJ, 519, L17
 Spruit, H. C., Daigne, F., & Drenkhahn, G. 2001, A&A, 369, 694
 Thompson, C. 1994, MNRAS, 270, 480
 Usov, V. V. 1994, MNRAS, 267, 1035
 Vlahakis, N., & Tsinganos, K. 1998, MNRAS, 298, 777
 Vlahakis, N., Tsinganos, K., Sauty, C., & Trussani, E. 2000, MNRAS, 318, 417
 Woods, E., & Loeb, A. 1995, ApJ, 453, 583